



Bisecting N-Acetylglucosamine Structures Inhibit Hypoxia-Induced Epithelial-Mesenchymal Transition in Breast Cancer Cells

Zengqi Tan¹, Chenxing Wang², Xiang Li^{1,3} and Feng Guan^{1*}

¹ College of Life Science, Northwest University, Xi'an, China, ² School of Biotechnology, Jiangnan University, Wuxi, China, ³ Wuxi Medical School, Jiangnan University, Wuxi, China

OPEN ACCESS

Edited by:

Chun Fang Gao,
Eastern Hepatobiliary Surgery
Hospital, China

Reviewed by:

Ayman A. Mohamed,
University of Illinois at
Urbana-Champaign, United States
Shujing Wang,
Dalian Medical University, China
Jenny Yuh-Jin Liang,
Chang Gung Memorial Hospital,
Institute of Stem Cell and Translational
Cancer Research, Taiwan

*Correspondence:

Feng Guan
guanfeng@nwu.edu.cn

Specialty section:

This article was submitted to
Clinical and Translational Physiology,
a section of the journal
Frontiers in Physiology

Received: 29 September 2017

Accepted: 23 February 2018

Published: 09 March 2018

Citation:

Tan Z, Wang C, Li X and Guan F
(2018) Bisecting N-Acetylglucosamine
Structures Inhibit Hypoxia-Induced
Epithelial-Mesenchymal Transition in
Breast Cancer Cells.
Front. Physiol. 9:210.
doi: 10.3389/fphys.2018.00210

The epithelial-mesenchymal transition (EMT) process plays a key role in many biological processes, including tissue fibrosis, metastatic diseases, and cancer progression. EMT can be induced by certain factors, notably hypoxia, in the tumor microenvironment. Aberrant levels of certain N-glycans is associated with cancer progression. We used an integrated strategy (mass spectrometry in combination with lectin microarray analysis) to elucidate aberrant glycosylation in a hypoxia-induced EMT model using breast cancer cell lines MCF7 and MDA-MB-231. The model showed reduced levels of bisecting GlcNAc structures, and downregulated expression of the corresponding glycosyltransferase MGAT3. MGAT3 overexpression in MCF7 suppressed cell migration, proliferation, colony formation, expression of EMT markers, and AKT signaling pathway, whereas MGAT3 knockdown (shRNA silencing) had opposite effects. Our findings clearly demonstrate the functional role (and effects of dysregulation) of bisecting GlcNAc structures in hypoxia-induced EMT, and provide a useful basis for further detailed studies of physiological functions of these structures in breast cancer.

Keywords: hypoxia, EMT, MGAT3, bisecting GlcNAc structures, breast cancer

INTRODUCTION

Breast cancer comprises ~30% of new cancer diagnoses, and is one of the most common causes of cancer mortality in women (Siegel et al., 2017). Many (25–40% of) invasive breast cancers contain hypoxic regions (Lundgren et al., 2007). Hypoxia (low oxygen level) is a well-documented characteristic of the tumor microenvironment. In patients with various types of cancer, tumors under hypoxic conditions were associated with increased metastasis and poor survival (Höckel and Vaupel, 2001). Most cellular responses to hypoxia are regulated by hypoxia-inducible factor-1 α (HIF-1 α) (Keith and Simon, 2007). HIF-1 is a heterodimer, which is consist of hypoxic response factor HIF-1 α and the constitutively expressed HIF-1 β . In normoxia, HIF-1 α is modified by prolyl hydroxylase, and hydroxylated HIF1 α is bound to the Von Hippel-Lindau (VHL) complex. VHL mediates the ubiquitylation of HIF-1 α , and contribute to degradation of HIF-1 α . In hypoxia, HIF-1 remains stable, and stabilized HIF-1 α is translocated to the nucleus, where it binds to hypoxia-response elements (HREs) and activates expression of hypoxia-response genes that control cellular processes such as energy metabolism, neovascularization, survival, pH, and migration (Pouyssegur et al., 2006).

Hypoxia has also been shown to induce the epithelial-mesenchymal transition (EMT) process (Liu L. et al., 2014; Liu Y. et al., 2014). Epithelial cells that undergo EMT are characterized by loss of cell-cell adhesion and cell polarity, and acquisition of migratory and invasive properties, and become involved in wound healing, tissue regeneration, organ fibrosis and tumor progression (Marcucci et al., 2016). Numerous studies have demonstrated functional roles and altered levels of glycans and their glycoconjugates in EMT and various other physiological and pathological processes. Reduced levels of β 4GalT4 gene and its product ganglioside GM4 were observed during transforming growth factor (TGF β)-induced EMT in normal mouse mammary epithelial NMuMG cells (Guan et al., 2009). Expression of N-acetylglucosaminyltransferase III (GnT-III, also known as MGAT3) and its products (bisecting GlcNAc structures) were suppressed in TGF β -induced EMT (Xu et al., 2012; Tan et al., 2014). Bisecting GlcNAc structures were present in membrane proteins of serous ovarian cancer cells but not of non-cancerous ovarian surface epithelial cells (Anugraham et al., 2014). MGAT3 expression was upregulated in brains of Alzheimer's disease patients (Akasaka-Manya et al., 2010).

Bisecting GlcNAc structure, a modification found in complex and hybrid N-glycans, results from attachment of N-acetylglucosamine (GlcNAc) to core mannose of the N-glycan via β 1,4 linkage, catalyzed by MGAT3. Bisecting GlcNAc structures play regulatory roles in biosynthesis of N-glycans, and their presence suppresses continued processing or elongation of N-glycans catalyzed by other glycosyltransferases (e.g., GnT-II, GnT-IV, GnT-V) (Xu et al., 2011, 2012; Lu et al., 2016). GnT-V and its products (β 1,6-branched N-glycans) were positively correlated with tumor cell metastasis, whereas MGAT3, as an antagonist of GnT-V, suppressed metastasis (Gu and Taniguchi, 2008; Gu et al., 2009). MGAT3 and bisecting GlcNAc structures participate in processes such as differentiation and carcinogenesis by regulating functions of target glycoproteins. In previous studies, MGAT3 expression was positively regulated by E-cadherin/ β -catenin-mediated signaling, and negatively regulated by Wnt/ β -catenin signaling (Iijima et al., 2006; Akama et al., 2008; Xu et al., 2011, 2012). MGAT3 modified N-glycosylation of epithelial growth factor receptor (EGFR) and integrin, and inhibited cell surface binding of EGFR/integrin to galectin-3, resulting in their endocytosis, suppression of intracellular signaling, and consequent promotion of cell migration and tumor metastasis (Partridge et al., 2004).

In the present study, we investigated (i) levels of bisecting GlcNAc structures and their inhibitory effects during hypoxia-induced EMT in breast cancer cell lines, using high-throughput techniques (mass spectrometry, lectin microarray), and (ii) effects of MGAT3 on cell proliferation, migration, colony formation, and signaling pathways. Hypoxia as a common feature of most tumors, contributes to chemoresistance, radioresistance, angiogenesis, vasculogenesis, invasiveness, and metastasis. Tumor hypoxia might be considered the best validated target. Our findings showed that bisecting GlcNAc structures retarded the EMT progression induced by hypoxia, which suggested the therapeutic potential of enhancing MGAT3 as a treatment for controlling breast cancer development.

MATERIALS AND METHODS

Cell Lines and Culture

Human breast cancer MCF7 and MDA-MB-231 cell lines were from American Type Culture Collection (ATCC; Manassas, VA, USA). Cells were cultured in DMEM supplemented with 10% fetal bovine serum (Biological Industries; Kibbutz Beit Haemek, Israel) and 1% penicillin-streptomycin (Gibco; Carlsbad, CA, USA) at 37°C in 5% CO₂ atmosphere as described in other study (Mertens-Talcott et al., 2007; Kim et al., 2010; Wardi et al., 2014). For hypoxic treatment, cells were maintained in an *in vivo* 200 hypoxia chamber (Ruskin; Bridgend, UK) with 1% O₂/ 5% CO₂/ 94% N₂ atmosphere for 24 h as previously described (Nagpal et al., 2015; He et al., 2017).

Total Protein Extraction

Total proteins were extracted with T-PER Reagent (Thermo Scientific; San Jose, CA) as described previously (Tan et al., 2014). In brief, cells ($\sim 1 \times 10^7$) were detached with trypsin, washed twice with ice-cold $1 \times$ PBS (0.01 M phosphate buffer containing 0.15 M NaCl, pH 7.4), lysed with 1 mL T-PER Reagent containing protease inhibitor cocktail (Sigma-Aldrich; St. Louis, MO, USA) and phosphatase inhibitor cocktail (Sigma-Aldrich), incubated for 30 min on ice, homogenized, and centrifuged at 12,000 rpm for 15 min. The supernatant was collected and stored at -80°C . Protein concentration was determined by BCA assay (Beyotime; Haimen, Jiangsu, China).

Western Blotting

Western blotting was performed as described previously (Tan et al., 2014). In brief, total proteins (30 μg) from normoxia- and hypoxia-treated samples were separated by 7.5% SDS-PAGE. Gels were transferred onto polyvinylidene difluoride (PVDF) membranes with Trans-Blot Turbo Transfer System (Bio-Rad; Hercules, CA). Membranes were soaked in 5% skim milk in TBST (20 mM Tris-HCl, 150 mM NaCl, 0.05% Tween 20, pH 8.0) for 2 h at 37°C, probed with primary antibodies against MGAT3 (1:500; ab135514; Abcam, Cambridge, MA, UK), fibronectin (1:1000; ab2413; Abcam), E-cadherin (1:10000; 610181; BD Biosciences, San Jose, CA, USA), β -catenin (1:5000; ab32572; Abcam), tubulin (1:5000; T7816; Sigma-Aldrich, St. Louis, MO, USA), HIF-1 α (1:1000; 3716; Cell Signaling Technology, Beverly, MA, USA), GLUT1 (1:5000; ab40084; Abcam), AKT (pan) (1:1000; 4685; Cell Signaling Technology), and p-AKT (Ser473) (1:2000; 4060; Cell Signaling Technology) overnight at 4°C and incubated with appropriate HRP-conjugated secondary antibody. Specific bands were visualized with a Pro-light HRP Kit (Tiangen; Beijing, China).

Wound Healing Assay

Wound healing assay was performed as described previously (Castro et al., 2018). Migratory capacity of cells was determined by wound healing assay. In brief, cells (2×10^5 per well, in a six-well plate) were cultured overnight and treated as described above. Three separate wounds were scratched with a pipette tip on the cell monolayer in each well, moving perpendicularly to a line drawn at the bottom of the plate. Cells were rinsed twice with $1 \times$ PBS twice, added with fresh serum-free medium, and wounds

at marked lines were photographed. After 24 h incubation at 37°C under normoxia or hypoxia, cells were washed with ice-cold 1× PBS, and wound tracks were photographed and marked using ImagePro Plus software (Media Cybernetics; Silver Spring, MD, USA).

Cell Proliferation

Cell proliferation was performed as described previously (Yu et al., 2008). Cells were plated in 96-well plates, and incubated 4 h with CellTiter 96 AQueous. One Solution Cell Proliferation Assay (MTS) solution (Promega; Madison, WI, USA). MTS products in supernatant were transferred into 96-well microtiter plates, and absorbance at 490 nm was determined.

Colony Formation

Colony formation was performed as described previously (Yu et al., 2008). Cells (2,500 per well) were plated in a 6-cm dish, and grown 1–2 weeks until small colonies were clearly seen. Medium was discarded, cells were rinsed twice with 1× PBS, fixed with 2% fresh paraformaldehyde, stained with crystal violet solution, and photos were taken. 10% acetic acid solution (1 mL) was added to dissolve the crystal violet. Optical density at 595 nm (OD 595) was measured.

RNA Isolation

RNA isolation was performed as described previously (Tan et al., 2014). Cells (1×10^5 per well in a six-well plate) were cultured and treated as described above. Total RNA was isolated using an RNeasy Tissue Kit (QIAGEN; Beijing) as per the manufacturer's instructions.

Quantitative Real-Time PCR

Real-time PCR was performed as described previously (Tan et al., 2014). Total RNA was extracted as above. Primers were selected from qPrimerDepot (primerdepot.nci.nih.gov/) (Cui et al., 2007). First-strand cDNA was synthesized from total RNA using a ReverTra Ace- α First-strand cDNA Synthesis Kit (Toyobo; Osaka, Japan). Quantitative real-time PCR was performed by LightCycler-based SYBR Green I dye detection with UltraSYBR Mixture (QIAGEN). Gene expression was quantified by the $2^{-\Delta\Delta CT}$ method (Livak and Schmittgen, 2001).

Lectin Microarray Analysis

Lectin microarrays were constructed and analyzed as described previously (Qin et al., 2012; Yu et al., 2012). In brief, 37 commercial lectins from Vector Laboratories (Burlingame, CA), Sigma-Aldrich, and Calbiochem Merck (Darmstadt, Germany) were immobilized onto a solid support at high spatial density. Glycoprotein samples labeled with fluorescent dye Cy3 (GE Healthcare; Buckinghamshire, UK) were applied to the lectin microarrays, and the arrays were scanned with a GenePix 4000B confocal scanner (Axon Instruments; Union City, CA).

Lectin Staining

Lectin staining was performed as described previously (Tan et al., 2014). Cells were cultured in 24-well plates with sterilized coverslips to obtain monolayers with 70–80% confluence. Cells were washed with ice-cold 1× PBS, immobilized with 2%

fresh paraformaldehyde for 15 min at room temperature (RT), permeabilized with 0.2% Triton X-100 in 1× PBS for 10 min at RT, and blocked with 5% BSA in 1× PBS for 1 h at 37°C. Fixed cells were incubated with 15–20 $\mu\text{g}/\text{mL}$ Cy3 fluorescein-labeled lectins (Con A, MAL-I, LCA, PHA-E) in 5% BSA for 3 h in the dark at RT, washed with 1× PBS, stained with 20 $\mu\text{g}/\text{mL}$ DAPI in 1× PBS for 10 min at RT, washed again with 1× PBS, and photographed with a fluorescence microscope (model Eclipse E600; Nikon; Tokyo, Japan).

N-Glycan Separation

N-glycans were separated as described previously (Tan et al., 2014). In brief, total proteins (2 mg) from each cell line were concentrated and desalted using a size-exclusion spin ultrafiltration unit (Amicon Ultra-0.5 10 KD, Millipore; Billerica, MA). Proteins were denatured with 8 M urea, 10 mM DTT, and 10 mM IAM (Sigma-Aldrich) and centrifuged. The sample was further digested with PNGase F (New England BioLabs; Ipswich, MA) overnight at 37°C. Released N-glycans were collected and lyophilized.

Desalting of N-Glycans

N-glycans were desalted as described previously (Tan et al., 2014). N-glycans were desalted using Sepharose 4B (Sigma-Aldrich) as described previously (Tan et al., 2014). In brief, Sepharose 4B in a microtube was pre-equilibrated with methanol/ H₂O (1:1 v/v) (MW) and 1-butanol/ methanol/ H₂O (5:1:1 v/v/v) (BMW). Glycans were dissolved in 500 μL BMW, added to the Sepharose 4B, and the mixture was shaken gently and washed with BMW. N-glycans were eluted with MW, and the eluent was collected and lyophilized.

Mass Spectrometry

Mass spectrometry analysis of N-glycans was performed as described previously (Tan et al., 2014). N-glycans were characterized by MALDI-TOF-MS (UltrafleXtreme, Bruker Daltonics; Bremen, Germany). Lyophilized N-glycans were resuspended in 10 μL MW, and 1 μL of the mixture was spotted onto an MTP AnchorChip sample target and air-dried. 1 μL of 20 mg/mL 2, 5-dihydroxybenzoic acid (DHB) in MW was spotted to recrystallize the glycans. Measurements were taken in positive-ion mode, and m/z data were analyzed and N-glycan structures were annotated using the GlycoWorkbench software program (code.google.com/p/glycoworkbench/). Relative intensity was analyzed and generated using FlexAnalysis software (Bruker Daltonics) based on MALDI-TOF-MS intensity. Relative proportion was calculated by accumulating the relative intensity of a given type N-glycan.

Overexpression and Knockdown of MGAT3 in MCF7 Cells

MGAT3 was amplified via PCR and linked to lentiviral overexpression vector pLVX-AcGFP1-N1 (Takara; Shiga, Japan). Lentiviral shRNA vector is constructed based on pLVX-shRNA2-Puro (Takara). Target sequences are listed below. Lentiviral vectors were packed in HEK293T via the packaging system, together with pMD2.G and psPAX2 (Addgene; Cambridge, MA,

USA). Transfected MCF7 cells were selected and enriched by adding puromycin to culture medium.

	Sequence
Target1	TGTATGGGCTGGACGGCAT
Target2	CCCAACTTCAGACAGTATGA

Statistical Analysis

Data are presented as mean \pm SD. Statistical significance of differences between means was evaluated by Student's *t*-test at $p < 0.05$.

RESULTS

Hypoxia Induces EMT and Increases Migration in Hypoxia-Treated Cells

Previous studies using various cancer cell models have demonstrated induction of EMT by hypoxic conditions (Zhou et al., 2009; Copple, 2010). In the present study, we exposed breast cancer cell lines MCF7 and MDA-MB-231 to hypoxic environments. HIF-1 α , an indicator of hypoxic conditions, was strongly expressed in hypoxia-treated cells (Figure 1A). The treated cells also showed loss of an epithelial character (E-cadherin) and acquisition of a mesenchymal character (fibronectin), typical hallmarks of EMT, and elevated expression of glucose transporter-1 protein (GLUT1), a putative intrinsic cellular marker of hypoxia regulated by HIF-1 α (Figure 1A).

Hypoxia treatment (1% O₂) of the two cell lines for 72 h resulted in altered morphology in comparison with normoxia (21% O₂) treated cells. Hypoxia-treated cells showed elongation and flattening (Figure 1B), and strongly enhanced migratory capacity, particularly in MCF7 (Figure 1C).

N-Glycan Profiles of Normoxia- and Hypoxia-Treated Cells

Alterations in glycosylation have been observed in numerous physiological and pathological processes. To identify specific N-glycan alterations during hypoxia, we used MALDI-TOF-MS to compare glycomic profiles of normoxia- vs. hypoxia-treated cells. Compositional and structural features were indicated in representative MALDI-TOF-MS spectra with signal-to-noise ratios >5 (Figures 2, 3, Tables S1, S2; Supplementary Information).

Thirty-four individual N-glycan masses were detected in MCF7, and 19 in MDA-MB-231. Numbers of distinct N-glycans were: 33 in normoxia-treated MCF7, 25 in hypoxia-treated MCF7, 17 in normoxia-treated MDA-MB-231, and 16 in hypoxia-treated MDA-MB-231. N-glycan structures found exclusively under hypoxic conditions in each of the two cell lines were mostly complex or hybrid type rather than high-mannose type.

We examined quantitative differences in various N-glycan types under the two conditions, as shown by the relative proportions summarized in Table 1. Proportions of bisecting GlcNAc structures were reduced under hypoxia vs. normoxia

(2.51 vs. 5.35% in MCF7; 3.62 vs. 5.65% in MDA-MB-231). Proportions under hypoxia vs. normoxia were also reduced for hybrid type N-glycans (2.94 vs. 4.34% in MCF7; 1.47 vs. 3.66% in MDA-MB-231) and for sialylation (0.43 vs. 0.76% in MCF7; 0.00 vs. 3.02% in MDA-MB-231). Proportions for fucosylation under hypoxia vs. normoxia were elevated in MCF7 (22.57 vs. 17.03%) but reduced in MDA-MB-231 (13.58 vs. 21.62%). Detailed information regarding substituents and branching patterns of N-glycans was obtained by MALDI-TOF/TOF-MS/MS (Figure S1).

Glycopattern Alteration in Hypoxia-Treated Cells

Lectin microarray analysis was used to identify specific glycopatterns in hypoxia-treated vs. normoxia-treated cells. The microarray was used to analyze fine glycan structures of glycoproteins in cells under the two conditions contained 37 lectins (Table S3), including two negative controls (BSA) and one positive control (Cy3-BSA). Under hypoxia, significant differences (>1.5 -fold or <0.67 -fold) were observed for glycans recognized by 12 different lectins in MCF7 and by 22 different lectins in MDA-MB-231 (Figure 4A). In both cell lines, bisecting GlcNAc structures (recognized by PHA-E), core fucosylation (recognized by PSA), and T antigen (recognized by PNA) were significantly suppressed, whereas non-substituted α 1,6-Man structures (recognized by HHL) was elevated (Tables 2, 3). A heatmap produced by complete hierarchical clustering and visualization using the HemI 1.0 software program (hemio.bio.cuckoo.org/down.php) (Deng et al., 2014) showed side-by-side clustering of normoxia- and hypoxia-treated cells in the dendrogram for both MCF7 and MDA-MB-231 (Figure 4A).

Glycan profiles under hypoxic conditions were further investigated and confirmed by histochemistry using PHA-E, MAL-I, LCA, and Con A (Figure 4B). Both MCF7 and MDA-MB-231 showed strong reduction of PHA-E and increase of Con A fluorescence signals. MCF7 showed reduction of MAL-I and MDA-MB-231 showed reduction of LCA signals, consistently with results of lectin microarray analysis. On the other hand, MDA-MB-231 microarray results using Con A were inconsistent with the elevated high-mannose N-glycan levels detected by mass spectrometry, lectin histochemistry, and microarray results using NPA and HHL. This apparent discrepancy may be due to random orientation of Con A following immobilization on glass slides (Qin et al., 2012). We examined expression of MGAT3 (which catalyzes synthesis of bisecting GlcNAc structures) in hypoxia-treated MCF7 and MDA-MB-231, and found that it was decreased at protein level (Figure 4C).

Overexpression of MGAT3 Inhibits Hypoxia-Induced EMT in MCF7 Cells

To elucidate the functional effects of reduced levels of bisecting GlcNAc structures and MGAT3 during hypoxia, we overexpressed *MGAT3* gene in MCF7. Cells were stably transduced with a green fluorescent protein (GFP)-marked lentivirus carrying mock (MCF7/mock) or *MGAT3* (MCF7/MGAT3-1/2). *MGAT3* overexpression was confirmed by western blotting (Figure 5A) and PHA-E lectin blotting

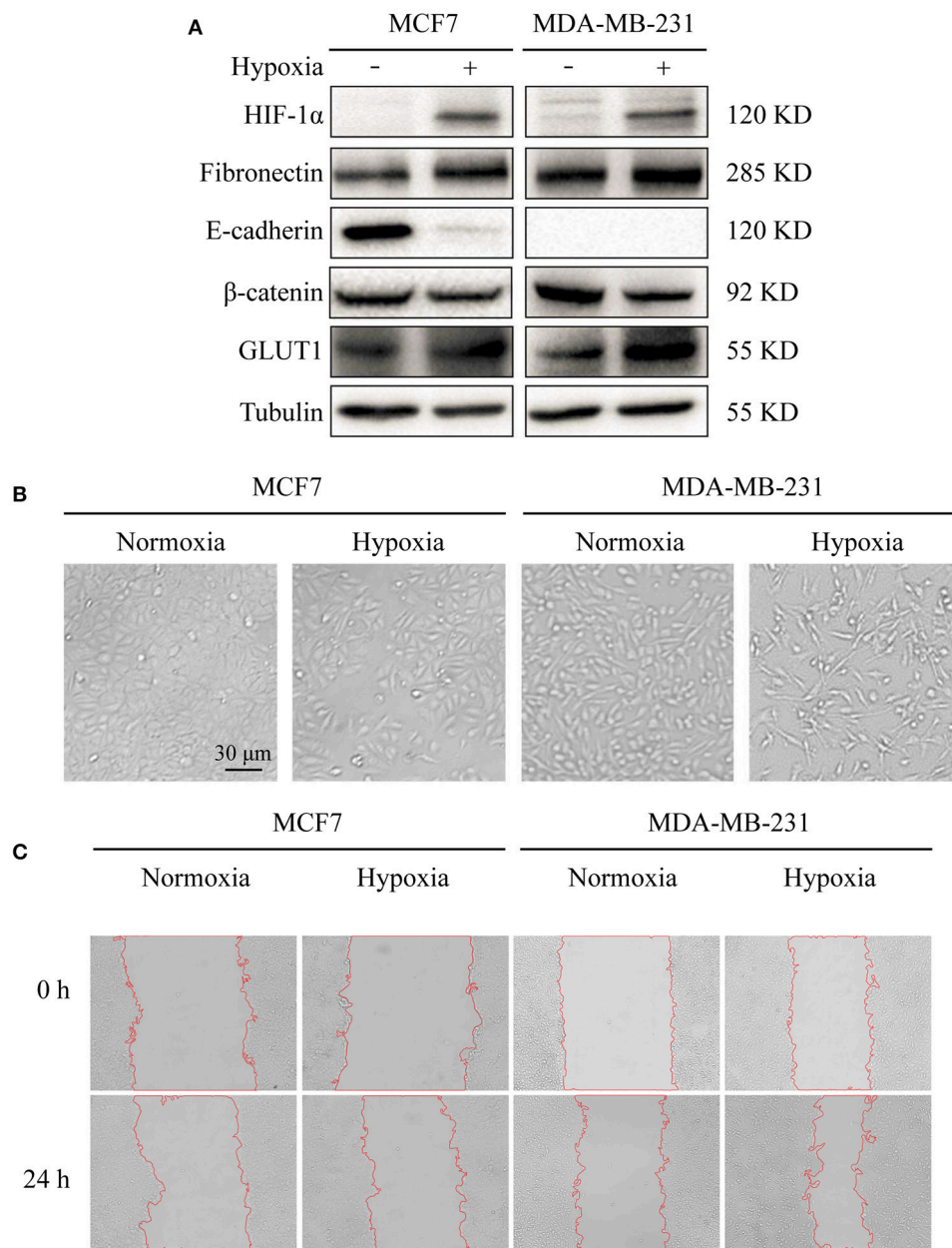
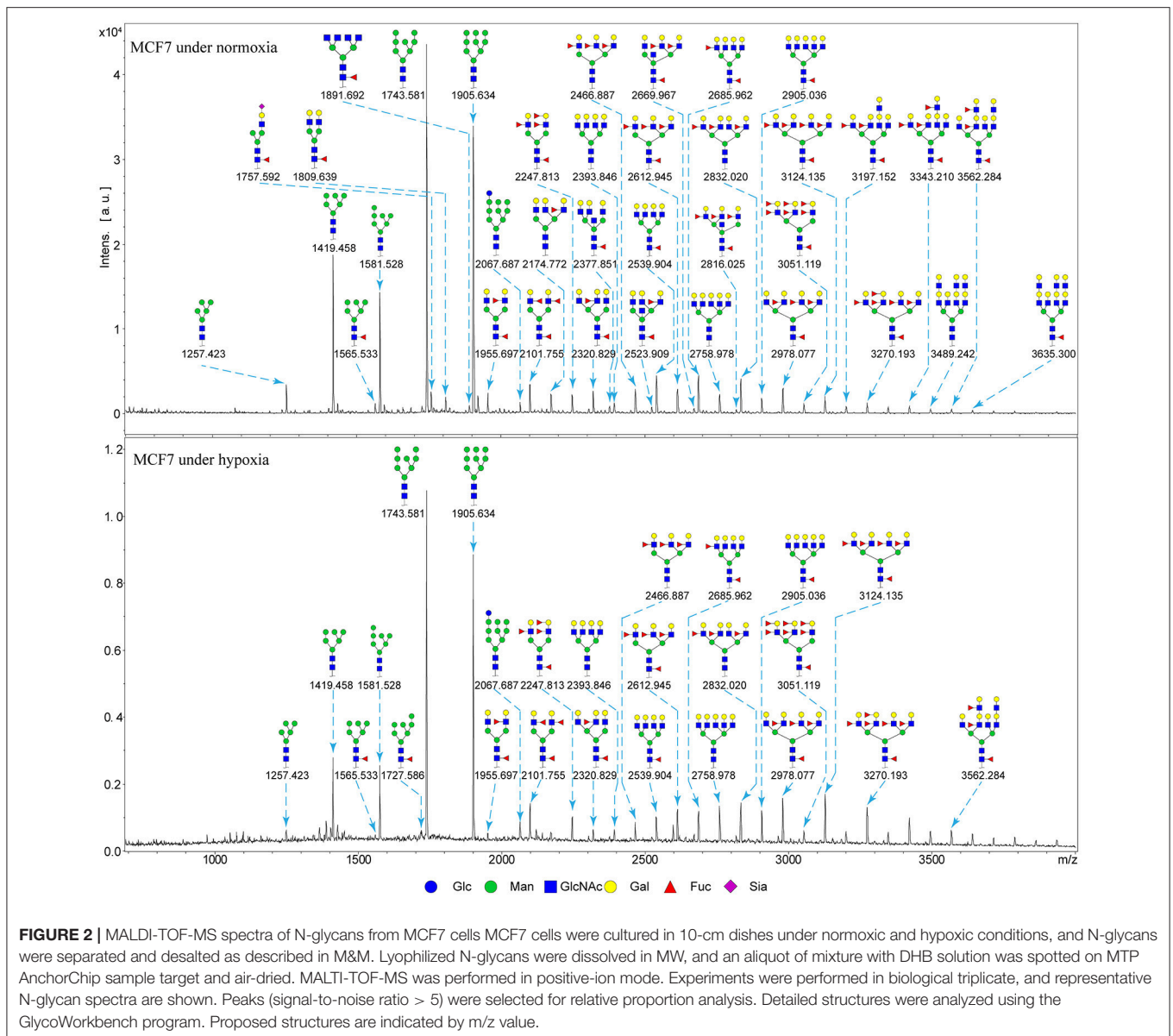


FIGURE 1 | Effects of hypoxia on cell markers, morphology, and migration **(A)** Expression in breast cancer MCF7 and MDA-MB-231 cells of E-cadherin (epithelial marker), fibronectin (epithelial marker), HIF-1 α (hypoxia marker), β -catenin, and GLUT1. Cells were cultured at 37°C in 5% CO₂ atmosphere for normoxic treatment, and in 1% O₂/ 5% CO₂/ 94% N₂ atmosphere for hypoxic treatment. Cells were harvested, lysed in T-PER Reagent, and protein content was determined by BCA assay. Western blotting was performed as described in M&M. **(B)** Morphological changes under normoxic and hypoxic conditions. Cells (2×10^5 per well) were grown in 6-well plates for 24 h under the two conditions. Photos were taken by phase-contrast microscopy at 200 \times magnification. **(C)** Cell migration assessed by wound assay. Cell monolayers under the two conditions were scratched with pipette tip. Cells were washed with ice-cold 1 \times PBS and cultured in serum-free medium. Pictures of wounds were taken at 0 and 24 h by phase-contrast microscopy (100 \times magnification).

(**Figure 5B**), and resulted in increased expression of MGAT3 and bisecting GlcNAc structures. The elevation of MGAT3 level inhibited proliferation (**Figure 5C**), colony formation (**Figures 5D,E**), and migration (**Figures 5F,H**) of the cells.

Previous studies have shown that MGAT3 regulates activation of signaling pathways such as extracellular signal-regulated

kinase (ERK) 1/2 or protein kinase B (AKT) (Miwa et al., 2013), and is involved in EMT and its reversed process, mesenchymal-epithelial transition (MET) (Pinho et al., 2012; Xu et al., 2012). We therefore examined possible effects of aberrant MGAT3 expression on relevant signaling pathway during hypoxia. In mock transfectants under hypoxia, reduced



E-cadherin expression, increased fibronectin expression, and activation of AKT signaling were observed (**Figure 5G**). In MGAT3 transfectants under hypoxia, MGAT3 overexpression had significant blocking effects on downregulation of E-cadherin expression, upregulation of HIF-1 α expression, and AKT signaling activation, and a slight blocking effect on upregulation of fibronectin expression (**Figure 5G**). These findings, taken together, indicate that MGAT3 overexpression inhibits hypoxia-induced EMT.

MGAT3 Knockdown Promote Hypoxia-Induced EMT in MCF7

We silenced MGAT3 expression in MCF7 using MGAT3 shRNAs (MCF7/shMGAT3-1/2) or shNC (MCF7/shNC). MGAT3 knockdown was confirmed by western blotting

(**Figure 6A**). Cell proliferation and migration were enhanced in MGAT3-shRNA transfectants (**Figures 6B,C,E**). Under hypoxia, MGAT3 knockdown in these cells promoted downregulation of E-cadherin expression and AKT signaling activation, but had no notable effect on β -catenin expression (**Figure 6D**).

DISCUSSION

Hypoxic regions, arising from irregular blood flow, chaotic vasculature, and/or poor oxygen diffusion, are present throughout solid cancer tissues (Jiang et al., 2011). Whereas hypoxia is toxic to normal cells, genetic and adaptive changes that occur in cancer cells allow them to survive and proliferate under hypoxic conditions. Such processes are the basis of malignant phenotype and aggressive tumor behavior. HIF-1/2 activation

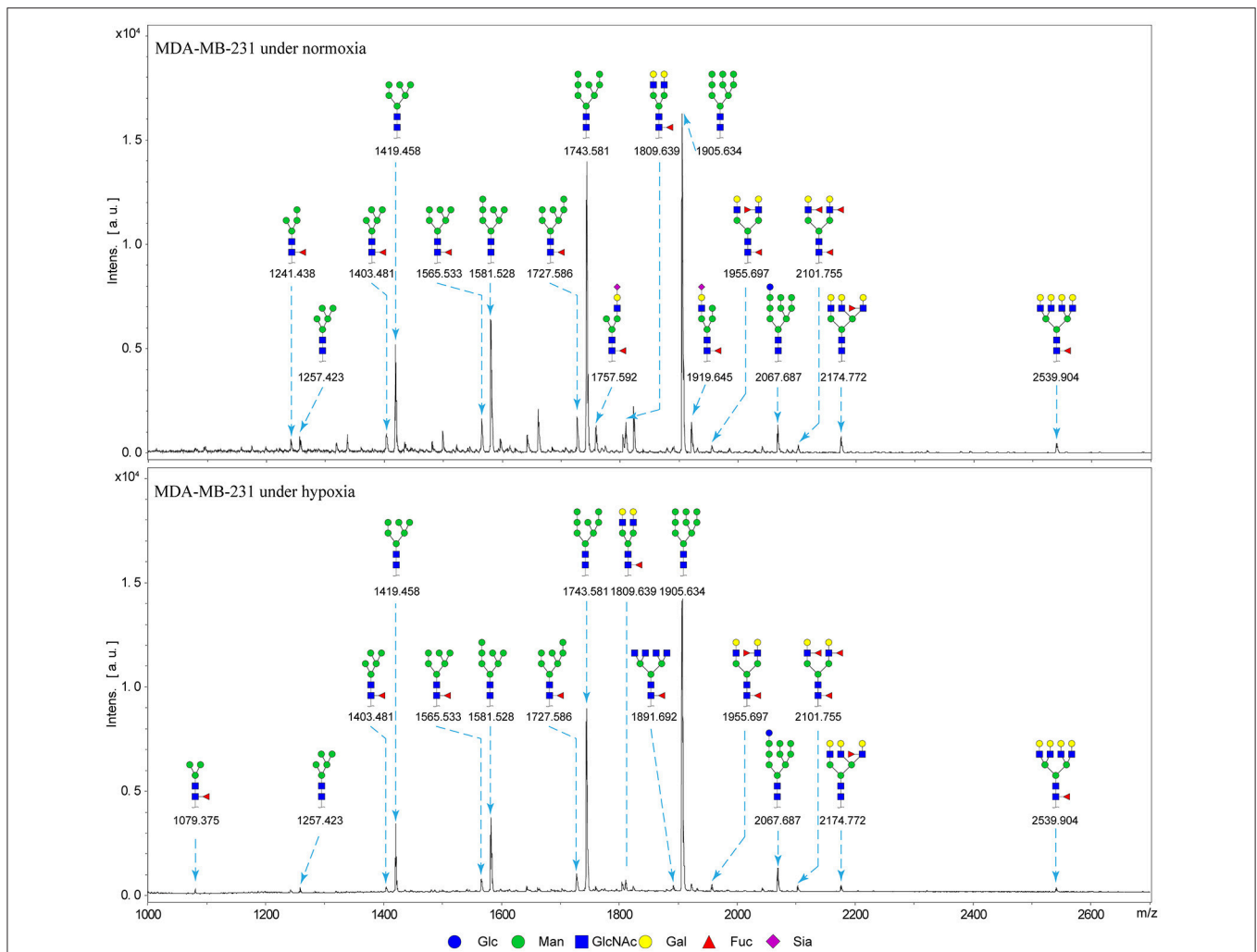


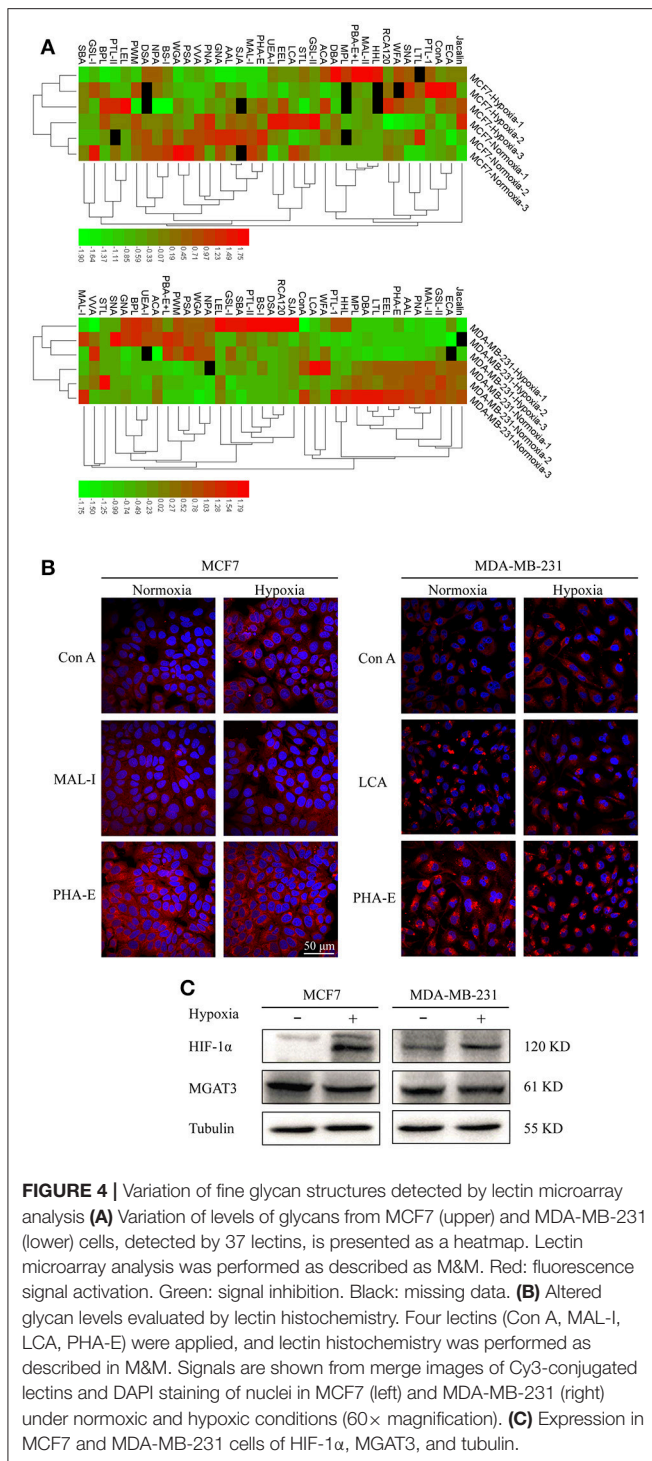
FIGURE 3 | MALDI-TOF-MS spectra of N-glycans from MDA-MB-231 cells. MDA-MB-231 cells were cultured in 10-cm dishes under normoxic and hypoxic conditions, and N-glycans were separated and desalted as described in M&M. Lyophilized N-glycans were dissolved in MW, and an aliquot of mixture with DHB solution was spotted on MTP AnchorChip sample target and air-dried. MALDI-TOF-MS was performed in positive-ion mode. Experiments were performed in biological triplicate, and representative N-glycan spectra are shown. Peaks (signal-to-noise ratio > 5) were selected for relative proportion analysis. Detailed structures were analyzed using the GlycoWorkbench program. Proposed structures are indicated by m/z value.

TABLE 1 | Relative proportions of various types of N-glycans in MCF7 and MDA-MB-231 cells under normoxia and hypoxia.

Glycan type	Relative proportion (%) of MCF7		Relative proportion (%) of MDA-MB-231	
	Normoxia	Hypoxia	Normoxia	Hypoxia
High-mannose	83.52 ± 0.54	77.91 ± 11.07	89.98 ± 2.21	95.10 ± 1.00
Hybrid	4.34 ± 0.54	2.94 ± 0.73	3.66 ± 1.34	1.47 ± 0.27
Complex	15.67 ± 0.57	21.46 ± 9.98	8.63 ± 1.00	4.90 ± 1.00
Multi-antennary	16.48 ± 0.54	22.09 ± 11.07	7.00 ± 0.41	4.90 ± 1.00
Bisecting GlcNAc	5.35 ± 0.11	2.51 ± 0.04	5.65 ± 1.23	3.62 ± 0.66
Sialylation	0.76 ± 0.58	0.43 ± 0.75	3.02 ± 2.61	0.00
Fucosylation	17.03 ± 0.19	22.57 ± 8.31	21.62 ± 3.35	13.58 ± 1.54

under hypoxic conditions in tumors is a key mechanism leading to tumor aggressiveness, metastasis promotion, and patient mortality (Harris, 2002; Semenza, 2002; Maxwell, 2005). Under hypoxic conditions, the tumor microenvironment activates major EMT-triggering pathways (e.g., TGFβ signaling, Notch signaling) that facilitate tumor growth and metastasis, and HIF modulates major transcription factors (e.g., TWIST, SNAIL, SLUG, SIP1, ZEB1) that regulate EMT (Jiang et al., 2011). Hypoxia and constitutive HIF expression were each shown to induce EMT (Higgins et al., 2008; Moen et al., 2009).

We used an integrated strategy (mass spectrometry in combination with lectin microarray analysis) to elucidate aberrant expression of N-glycans in breast cancer cells under hypoxia. Hypoxia-treated MCF7 cells showed reduced levels of bisecting GlcNAc structures and MGAT3 expression, and



elevated levels of multi-antennary structures and fucosylation. In the process of N-glycan biosynthesis, the enzymes MGAT3 (GnT-III), GnT-IV (generating multi-antennary structures with β 1-4-linked GlcNAc on Man α 1-3 arm), GnT-V (generating multi-antennary structures with β 1-6-linked GlcNAc on Man α 1-6 arm), and FUT8 (generating core fucosylation) are able to utilize biantennary structures as substrates for N-glycan

elongation, and formation of N-glycan structures is determined by interplay among these enzymes; e.g., bisecting GlcNAc structures catalyzed by MGAT3 inhibit further catalytic activity by FUT8 and GnT-V (Taniguchi and Kizuka, 2015). Reduced levels of bisecting GlcNAc structures and MGAT3 expression may promote elevated levels of multi-antennary structures and fucosylation. In hypoxia-treated MDA-MB-231, we observed reduced levels of bisecting GlcNAc and multi-antennary structures, and increased levels of high-mannose structures. These changes may reflect a blocked step in N-glycan synthesis that results in incomplete glycosylation in these cells during hypoxia.

MGAT3 was transfected into MCF7 to clarify the functional role of this enzyme and its products (bisecting GlcNAc structures) during hypoxia. E-cadherin expression was significantly decreased in mock-transfected cells, whereas the rate of such decrease was much lower in MGAT3-transfected cells. In previous studies, MGAT3 overexpression blocked downregulation of E-cadherin expression during TGF β -induced EMT (consistently with our findings), delayed E-cadherin turnover, and reduced E-cadherin release from the cell surface (Yoshimura et al., 1996; Xu et al., 2012).

In the present study, exogenous MGAT3 blocked upregulation of p-AKT expression during hypoxia (Figure 5G). Bisecting GlcNAc structures and MGAT3 were shown previously to modify N-glycosylation of target proteins and to inhibit or activate related signaling pathways. For example, attachment of bisecting GlcNAc structures to growth factor receptors slowed tumor progression by inhibiting activation of growth factor signaling (Song et al., 2010), and modification by MGAT3 of integrin N-glycosylation inhibited its ligand binding ability and consequent integrin-mediated signaling (Isaji et al., 2004). MGAT3-catalyzed addition of bisecting GlcNAc structures reduced levels of (poly)N-acetylactosamine (LacNAc) structures on growth factor receptors by inhibiting GnT-V and GnT-IV. These changes suppressed binding of growth factor receptors to galectin-3, which forms a galectin lattice on the cell surface for clustering of glycoproteins with LacNAc, and promotes constitutive endocytosis of growth factor receptors, thereby inhibiting downstream signaling and consequent cell proliferation and survival through suppression of Erk and AKT signaling (Partridge et al., 2004; Lau et al., 2007; Miwa et al., 2013), consistently with our findings (Figure 5G). Suppression of AKT signaling may inhibit EMT, proliferation, and metastasis (Grille et al., 2003). Overexpression of GnT-III in highly metastatic melanoma cells was associated with reduced metastasis potential, and MGAT3-transfected melanoma cell performed significantly suppressed lung metastasis (Taniguchi and Kizuka, 2015), which were consistent with our data. Moreover, MGAT3^{-/-} mice overexpressing the polyomavirus middle T (PyMT) oncogene under the control of the mouse mammary tumor virus (MMTV) promoter exhibited an increased tumor burden, increased migration and early metastasis to lung (Song et al., 2010). These studies were consistent with our data.

In the present study, MGAT3 overexpression blocked elevation of HIF-1 α expression during hypoxia (Figure 5G), possibly through inhibition of AKT signaling. HIF-1 α expression

TABLE 2 | Differential glycopatterns in normoxia- vs. hypoxia-treated MCF7 cells revealed by lectin microarray analysis.

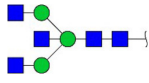


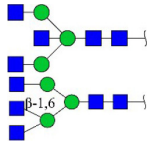
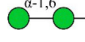
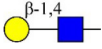
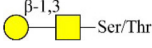
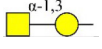
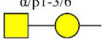
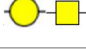
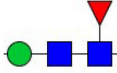
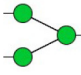
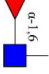
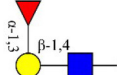
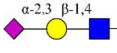
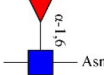
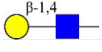
Lectin	Abbreviation	Specificity	FC of MCF7 (H/N)
<i>Maackia amurensis</i> lectin I	MAL-I	Gal β -1,4GlcNAc 	0.45
<i>Pisum sativum</i> agglutinin	PSA	Fuc α -N-acetylchitobiose-Man 	0.46
<i>Phaseolus vulgaris</i> erythroagglutinin	PHA-E	Bisecting GlcNAc 	0.60
Peanut agglutinin	PNA	Gal β 1-3GalNAc α -Ser/Thr(T) 	0.60
<i>Lotus tetragonolobus</i> lectin	LTL	Fuc α -1,3GlcNAc (core) 	1.61
<i>Concanavalin ensiformis</i> agglutinin	Con A	Branched and terminal Man 	1.61
Soybean agglutinin	SBA	Terminal GalNAc (especially GalNAc α 1-3Gal) 	1.74
<i>Maclura pomifera</i> lectin	MPL	α GalNAc 	6.65
<i>Phaseolus vulgaris</i> agglutinin	PHA-E+L	Bisecting GlcNAc and β -1,6-GlcNAc 	23.53
<i>Hippeastrum hybrid</i> lectin	HHL	Non-substituted α -1,6 Man 	54.63
<i>Maackia amurensis</i> lectin II	MAL-II	Sia α 2-3Gal β 1-4Glc(NAc) 	∞
<i>Psophocarpus tetragonolobus</i> lectin I	PTL-I	α GalNAc and Gal 	∞

TABLE 3 | Differential glycopatterns in normoxia- vs. hypoxia-treated MDA-MB-231 cells revealed by lectin microarray analysis.

Lectin	Abbreviation	Specificity	FC of MDA-MB-231 (H/N)
<i>Maackia amurensis</i> lectin I	GSL-II	Gal β -1,4GlcNAc 	0.00
Peanut agglutinin	PNA	Gal β 1-3GalNAc α -Ser/Thr(T) 	0.00
Soybean agglutinin	SBA	Terminal GalNAc (especially GalNAc α 1-3Gal) 	0.00
<i>Wisteria floribunda</i> agglutinin	WFA	GalNAc α / β 1-3/6Gal 	0.02
<i>Bandeiraea simplicifolia</i> lectin-I	BS-I	α -Gal, α -GalNAc 	0.06
<i>Pisum sativum</i> agglutinin	PSA	Fuc α -N-acetylchitobiose-Man 	0.09
Concanavalin A	Con A	Branched and terminal Man 	0.27
<i>Aleuria aurantia</i> lectin	AAL	Terminal Fuc α -1,6GlcNAc  Fuc α -1,3Gal β -1,4GlcNAc 	0.32
<i>Maackia amurensis</i> lectin II	MAL-II	Sia α 2-3Gal β 1-4Glc(NAc) 	0.34
<i>Lens culinaris</i> agglutinin	LCA	Fuc α -1,6GlcNAc (core) 	0.48
<i>Erythrina cristagalli</i> agglutinin	ECA	Gal β -1,4GlcNAc 	0.56

(Continued)

TABLE 3 | Continued

Lectin	Abbreviation	Specificity	FC of MDA-MB-231 (H/N)
<i>Psophocarpus tetragonolobus</i> lectin I	PTL-I	α GalNAc and Gal 	0.60
<i>Phaseolus vulgaris</i> erythroagglutinin	PHA-E	Bisecting GlcNAc 	0.60
<i>Narcissus pseudonarcissus</i> agglutinin	NPA	Non-substituted α -1,6 Man 	1.76
<i>Vicia villosa</i> agglutinin	VVA	GalNAc α -Ser/Thr(Tn) 	1.87
Jacalin	Jacalin	Gal β 1-3GalNAc α -Ser/Thr(TF)  GalNAc α -Ser/Thr(T) 	2.11
<i>Datura stramonium</i> agglutinin	DSA	GlcNAc 	2.33
<i>Solanum tuberosum</i> lectin	STL	(GlcNAc) _n 	128.47
<i>Griffonia simplicifolia</i> -lectin-I	GSL-I	α GalNAc, α Gal  GalNAc α -Ser/Thr(Tn) 	156.70
<i>Sophora japonica</i> agglutinin	SJA	Terminal GalNAc and Gal 	175.95
<i>Hippeastrum hybrid</i> lectin	HHL	Non-substituted α -1,6 Man 	251.86
<i>Euonymus europaeus</i> lectin	EEL	Gal α 1-3(Fuc α 1-2)Gal 	∞

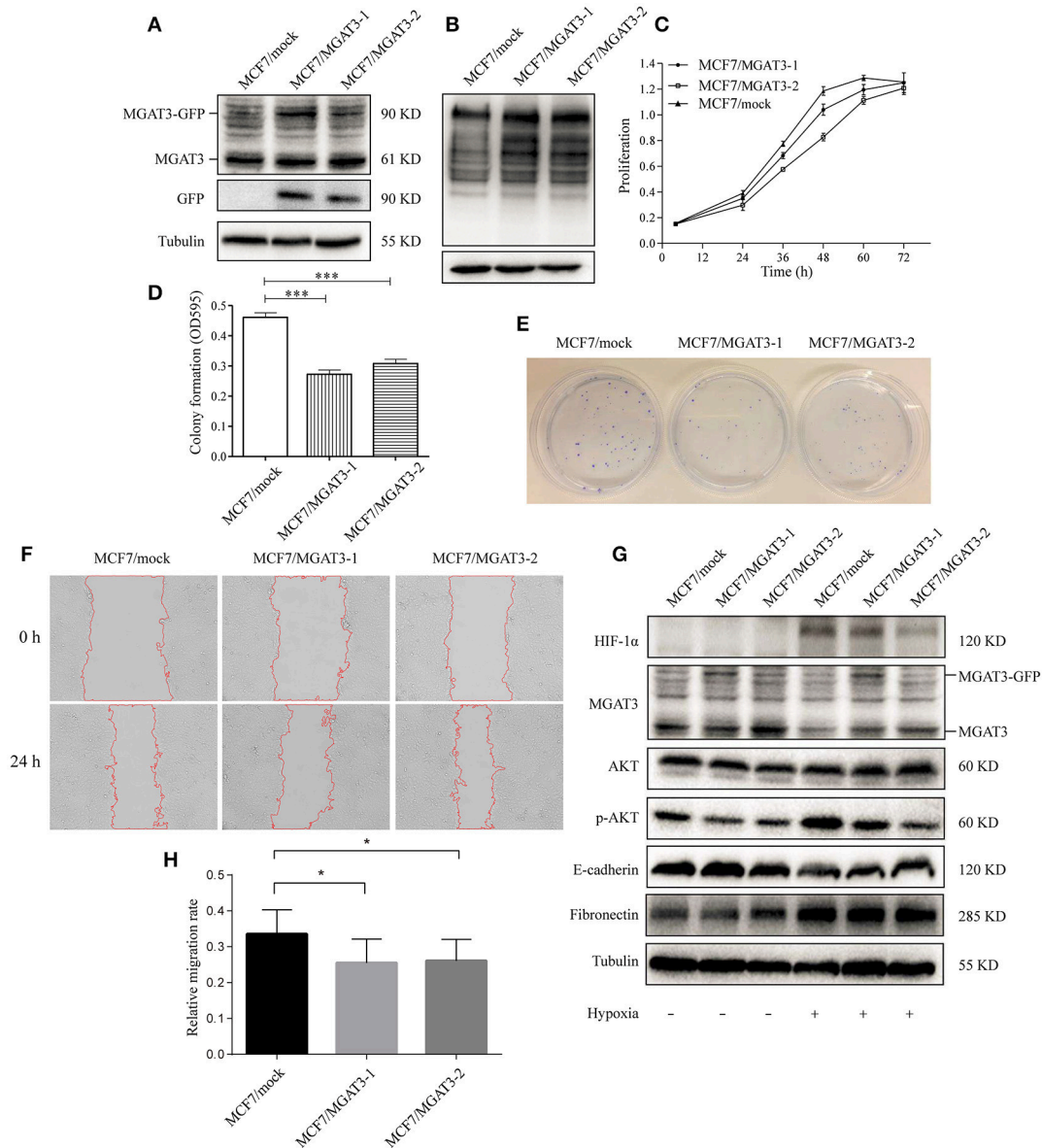
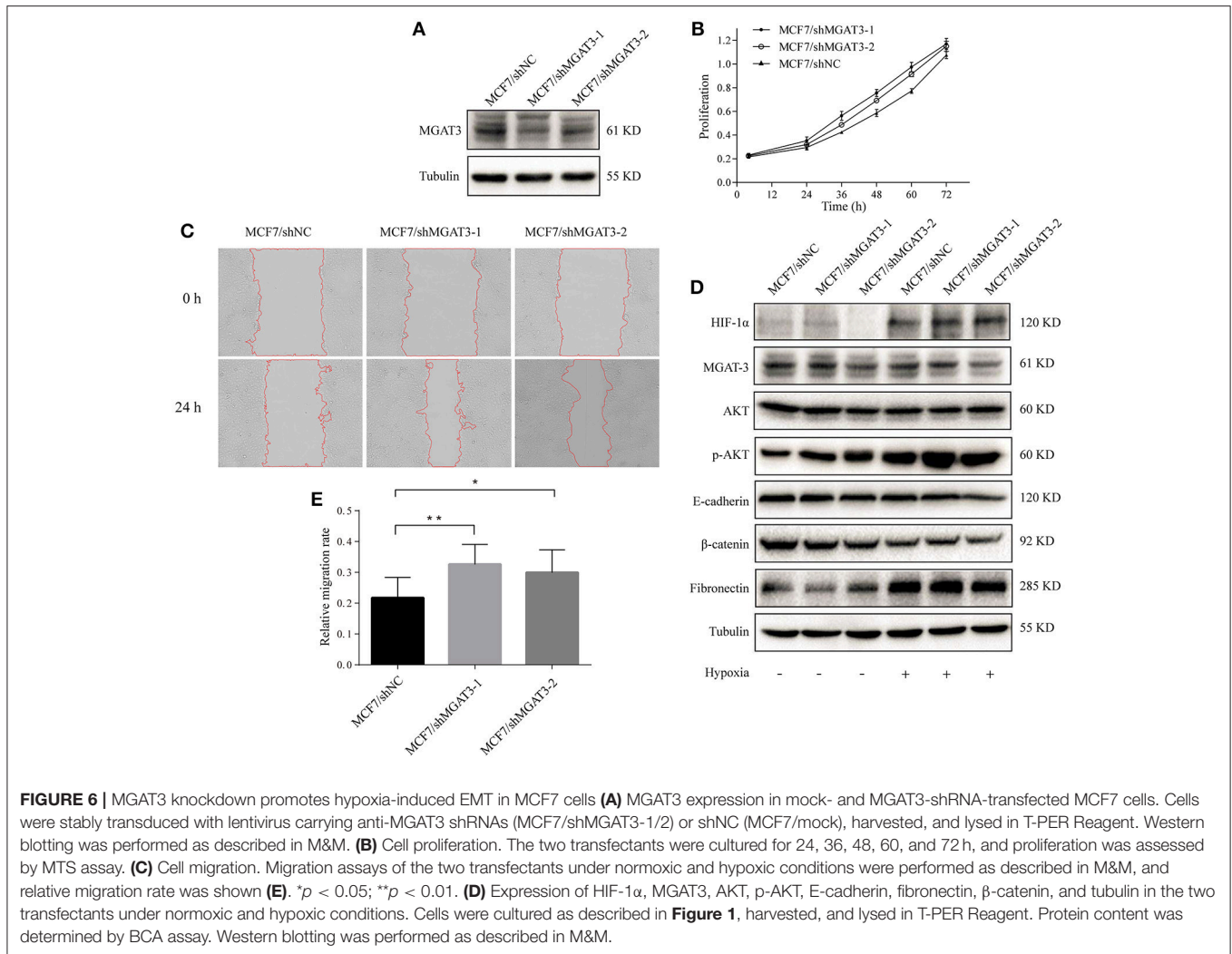


FIGURE 5 | MGAT3 overexpression suppresses hypoxia-induced EMT in MCF7 cells **(A)** MGAT3 expression in mock- and MGAT3-transfected MCF7 cells. Cells were stably transduced with a GFP-marked lentivirus carrying mock gene or MGAT3 gene, harvested, and lysed in T-PER Reagent. Western blotting was performed as described in M&M using anti-MGAT3 and anti-GFP antibody. **(B)** Levels of bisecting GlcNAc structures in mock- and MGAT3-transfectants. Whole cell lysates of the two transfectants were subjected to PHA-E lectin blotting as described in M&M. **(C)** Proliferation of transfectant cells. The two transfectants were cultured for 24, 36, 48, 60, and 72 h, and proliferation was assessed by MTS assay. **(E)** Colony formation ability. The two transfectants (2500 cells each) were cultured in 6-cm dishes for 1–2 week, fixed, stained with crystal violet solution, and photographed. Acetic acid was added to dissolve crystal violet, and OD 595 was determined **(D)**. $*p < 0.05$; $***p < 0.001$. **(F)** Cell migration. Migration assays of the two transfectants under normoxic and hypoxic conditions were performed as described in M&M, and relative migration rate was shown **(H)**. $*p < 0.05$. **(G)** Expression of HIF-1 α , MGAT3, AKT, p-AKT, E-cadherin, fibronectin, and tubulin in the two transfectants under normoxic and hypoxic conditions. Cells were cultured as described in **Figure 1**, harvested, and lysed in T-PER Reagent. Protein content was determined by BCA assay. Western blotting was performed as described in M&M.

may be regulated by PI3K/ PTEN/ AKT/ mTOR signaling (Zhong et al., 2000). Stimulation of Her2 activity by heregulin could also induce of HIF-1 α expression attributing to the 5'-untranslated region of HIF-1 α mRNA directing heregulin to express a heterologous protein (Laughner et al., 2001). HIF-1 α may affect hypoxia-induced EMT through TGF β signaling pathway by increasing SMAD3 mRNA levels and release of

latent TGF- β 2 (Zhang et al., 2003; Jiang et al., 2011). HIF-1 may also bind to and stabilize activated Notch, thereby affecting Notch signaling and hypoxia-induced EMT (Soares et al., 2004; Gustafsson et al., 2005; Jiang et al., 2011).

To further clarify the functional roles of bisecting GlcNAc structures and MGAT3 during hypoxia, we produced MGAT3-overexpressing and MGAT3 knockdown mutants of MCF7 cells.



Under hypoxic conditions, MGAT3 overexpression significantly blocked downregulation of E-cadherin expression, activation of AKT signaling, upregulation of HIF-1 α expression, and hypoxia-induced EMT. These observations were consistent with those from MGAT3 knockdown cells.

Hypoxia as a negative clinical prognostic indicator, is known to affect the response of solid malignancies to radiation and tumor oxygenation, and hypoxia is a strong predictor of both overall and disease-free survival. Our study indicated that MGAT3 might be a potential therapeutic target of hypoxic region of breast cancer. However, this study was deficient in molecular mechanism and *in vivo* experiments. Our ongoing studies include the exploration of the genetic and epigenetic bases of aberrant MGAT3 expression in breast cancer, and identification of target proteins bearing bisecting GlcNAc structures, and validation these results *in vivo* with the mouse model, and will clarify the detailed mechanism whereby these structures inhibit hypoxia-induced EMT in breast cancer cells.

AUTHOR CONTRIBUTIONS

FG, XL, and ZT: Designed experiments; CW and ZT: Carried out experiments; ZT: Analyzed experiments results; FG, XL, CW, and ZT: Wrote the manuscript.

ACKNOWLEDGMENTS

This study was supported by the National Natural Science Foundation of China (No. 81672537 and 81470294) and Hundred-Talent Program of Shaanxi Province. The authors are grateful to Dr. S. Anderson for English editing of the manuscript.

SUPPLEMENTARY MATERIAL

The Supplementary Material for this article can be found online at: <https://www.frontiersin.org/articles/10.3389/fphys.2018.00210/full#supplementary-material>

REFERENCES

- Akama, R., Sato, Y., Kariya, Y., Isaji, T., Fukuda, T., Lu, L., et al. (2008). N-acetylglucosaminyltransferase III expression is regulated by cell-cell adhesion via the E-cadherin-catenin-actin complex. *Proteomics* 8, 3221–3228. doi: 10.1002/pmic.200800038
- Akasaka-Manya, K., Manya, H., Sakurai, Y., Wojczyk, B. S., Kozutsumi, Y., Saito, Y., et al. (2010). Protective effect of N-glycan bisecting GlcNAc residues on β -amyloid production in Alzheimer's disease. *Glycobiology* 20, 99–106. doi: 10.1093/glycob/cwp152
- Anugraham, M., Jacob, F., Nixdorf, S., Everest-Dass, A. V., Heinzmann-Schwarz, V., and Packer, N. H. (2014). Specific glycosylation of membrane proteins in epithelial ovarian cancer cell lines: glycan structures reflect gene expression and DNA methylation status. *Mol. Cell. Proteomics* 13, 2213–2232. doi: 10.1074/mcp.M113.037085
- Castro, M. G., Campos, L. E., Rodriguez, Y. I., and Alvarez, S. E. (2018). *In vitro* methods to study the modulation of migration and invasion by sphingosine-1-phosphate. *Methods Mol. Biol.* 1697, 117–131. doi: 10.1007/7651_2017_51
- Copple, B. L. (2010). Hypoxia stimulates hepatocyte epithelial to mesenchymal transition by hypoxia-inducible factor and transforming growth factor- β -dependent mechanisms. *Liver Int.* 30, 669–682. doi: 10.1111/j.1478-3231.2010.02205.x
- Cui, W., Taub, D. D., and Gardner, K. (2007). qPrimerDepot: a primer database for quantitative real time PCR. *Nucleic Acids Res.* 35, D805–D809. doi: 10.1093/nar/gkl767
- Deng, W., Wang, Y., Liu, Z., Cheng, H., and Xue, Y. (2014). HemI: a toolkit for illustrating heatmaps. *PLoS ONE* 9:e111988. doi: 10.1371/journal.pone.0111988
- Grille, S. J., Bellacosa, A., Upson, J., Klein-Szanto, A. J., van Roy, F., Lee-Kwon, W., et al. (2003). The protein kinase Akt induces epithelial mesenchymal transition and promotes enhanced motility and invasiveness of squamous cell carcinoma lines. *Cancer Res.* 63, 2172–2178.
- Gu, J., Sato, Y., Kariya, Y., Isaji, T., Taniguchi, N., and Fukuda, T. (2009). A mutual regulation between cell-cell adhesion and N-glycosylation: implication of the bisecting GlcNAc for biological functions. *J. Proteome Res.* 8, 431–435. doi: 10.1021/pr800674g
- Gu, J., and Taniguchi, N. (2008). Potential of N-glycan in cell adhesion and migration as either a positive or negative regulator. *Cell Adh. Migr.* 2, 243–245. doi: 10.4161/cam.2.4.6748
- Guan, F., Handa, K., and Hakomori, S. I. (2009). Specific glycosphingolipids mediate epithelial-to-mesenchymal transition of human and mouse epithelial cell lines. *Proc. Natl. Acad. Sci. U.S.A.* 106, 7461–7466. doi: 10.1073/pnas.0902368106
- Gustafsson, M. V., Zheng, X., Pereira, T., Gradin, K., Jin, S., Lundkvist, J., et al. (2005). Hypoxia requires notch signaling to maintain the undifferentiated cell state. *Dev. Cell* 9, 617–628. doi: 10.1016/j.devcel.2005.09.010
- Harris, A. L. (2002). Hypoxia—a key regulatory factor in tumour growth. *Nat. Rev. Cancer* 2, 38–47. doi: 10.1038/nrc704
- He, C., Wang, L., Zhang, J., and Xu, H. (2017). Hypoxia-inducible microRNA-224 promotes the cell growth, migration and invasion by directly targeting RASSF8 in gastric cancer. *Mol. Cancer* 16:35. doi: 10.1186/s12943-017-0603-1
- Higgins, D. F., Kimura, K., Iwano, M., and Haase, V. H. (2008). Hypoxia-inducible factor signaling in the development of tissue fibrosis. *Cell Cycle* 7, 1128–1132. doi: 10.4161/cc.7.9.5804
- Höckel, M., and Vaupel, P. (2001). Tumor hypoxia: definitions and current clinical, biologic, and molecular aspects. *J. Natl. Cancer Inst.* 93, 266–276. doi: 10.1093/jnci/93.4.266
- Iijima, J., Zhao, Y., Isaji, T., Kameyama, A., Nakaya, S., Wang, X., et al. (2006). Cell-cell interaction-dependent regulation of N-acetylglucosaminyltransferase III and the bisected N-glycans in GE11 epithelial cells. Involvement of E-cadherin-mediated cell adhesion. *J. Biol. Chem.* 281, 13038–13046. doi: 10.1074/jbc.M601961200
- Isaji, T., Gu, J., Nishiuchi, R., Zhao, Y., Takahashi, M., Miyoshi, E., et al. (2004). Introduction of bisecting GlcNAc into integrin $\alpha 5 \beta 1$ reduces ligand binding and down-regulates cell adhesion and cell migration. *J. Biol. Chem.* 279, 19747–19754. doi: 10.1074/jbc.M311627200
- Jiang, J., Tang, Y. L., and Liang, X. H. (2011). EMT: a new vision of hypoxia promoting cancer progression. *Cancer Biol. Ther.* 11, 714–723. doi: 10.4161/cbt.11.8.15274
- Keith, B., and Simon, M. C. (2007). Hypoxia-inducible factors, stem cells, and cancer. *Cell* 129, 465–472. doi: 10.1016/j.cell.2007.04.019
- Kim, J. B., Yu, J. H., Ko, E., Lee, K. W., Song, A. K., Park, S. Y., et al. (2010). The alkaloid berberine inhibits the growth of anoikis-resistant MCF-7 and MDA-MB-231 breast cancer cell lines by inducing cell cycle arrest. *Phytomedicine* 17, 436–440. doi: 10.1016/j.phymed.2009.08.012
- Lau, K. S., Partridge, E. A., Grigorian, A., Silvescu, C. I., Reinhold, V. N., Demetriou, M., et al. (2007). Complex N-glycan number and degree of branching cooperate to regulate cell proliferation and differentiation. *Cell* 129, 123–134. doi: 10.1016/j.cell.2007.01.049
- Laughner, E., Taghavi, P., Chiles, K., Mahon, P. C., and Semenza, G. L. (2001). HER2 (neu) signaling increases the rate of hypoxia-inducible factor 1 α (HIF-1 α) synthesis: novel mechanism for HIF-1-mediated vascular endothelial growth factor expression. *Mol. Cell. Biol.* 21, 3995–4004. doi: 10.1128/MCB.21.12.3995-4004.2001
- Liu, L., Salmikov, A. V., Bauer, N., Aleksandrowicz, E., Labsch, S., Nwaeburu, C., et al. (2014). Triptolide reverses hypoxia-induced epithelial-mesenchymal transition and stem-like features in pancreatic cancer by NF- κ B downregulation. *Int. J. Cancer* 134, 2489–2503. doi: 10.1002/ijc.28583
- Liu, Y., Liu, Y., Yan, X., Xu, Y., Luo, F., Ye, J., et al. (2014). HIFs enhance the migratory and neoplastic capacities of hepatocellular carcinoma cells by promoting EMT. *Tumour Biol.* 35, 8103–8114. doi: 10.1007/s13277-014-2056-0
- Livak, K. J., and Schmittgen, T. D. (2001). Analysis of relative gene expression data using real-time quantitative PCR and the $2^{-\Delta\Delta C_T}$ method. *Methods* 25, 402–408. doi: 10.1006/meth.2001.1262
- Lu, J., Isaji, T., Im, S., Fukuda, T., Kameyama, A., and Gu, J. (2016). Expression of N-Acetylglucosaminyltransferase III suppresses $\alpha 2,3$ -sialylation, and its distinctive functions in cell migration are attributed to $\alpha 2,6$ -sialylation levels. *J. Biol. Chem.* 291, 5708–5720. doi: 10.1074/jbc.M115.712836
- Lundgren, K., Holm, C., and Landberg, G. (2007). Hypoxia and breast cancer: prognostic and therapeutic implications. *Cell. Mol. Life Sci.* 64, 3233–3247. doi: 10.1007/s00018-007-7390-6
- Marcucci, F., Stassi, G., and De Maria, R. (2016). Epithelial-mesenchymal transition: a new target in anticancer drug discovery. *Nat. Rev. Drug Discov.* 15, 311–325. doi: 10.1038/nrd.2015.13
- Maxwell, P. H. (2005). The HIF pathway in cancer. *Semin. Cell Dev. Biol.* 16, 523–530. doi: 10.1016/j.semcdb.2005.03.001
- Mertens-Talcott, S. U., Chintharlapalli, S., Li, X., and Safe, S. (2007). The oncogenic microRNA-27a targets genes that regulate specificity protein transcription factors and the G2-M checkpoint in MDA-MB-231 breast cancer cells. *Cancer Res.* 67, 11001–11011. doi: 10.1158/0008-5472.CAN-07-2416
- Miwa, H. E., Koba, W. R., Fine, E. J., Giricz, O., Kenny, P. A., and Stanley, P. (2013). Bisected, complex N-glycans and galectins in mouse mammary tumor progression and human breast cancer. *Glycobiology* 23, 1477–1490. doi: 10.1093/glycob/cwt075
- Moen, I., Øyan, A. M., Kalland, K. H., Tronstad, K. J., Aksten, L. A., Chekenya, M., et al. (2009). Hyperoxic treatment induces mesenchymal-to-epithelial transition in a rat adenocarcinoma model. *PLoS ONE* 4:e6381. doi: 10.1371/journal.pone.0006381
- Nagpal, N., Ahmad, H. M., Chameettachal, S., Sundar, D., Ghosh, S., and Kulshreshtha, R. (2015). HIF-inducible miR-191 promotes migration in breast cancer through complex regulation of TGF β -signaling in hypoxic microenvironment. *Sci. Rep.* 5:9650. doi: 10.1038/srep09650
- Partridge, E. A., Le Roy, C., Di Guglielmo, G. M., Pawling, J., Cheung, P., Granovsky, M., et al. (2004). Regulation of cytokine receptors by Golgi N-glycan processing and endocytosis. *Science* 306, 120–124. doi: 10.1126/science.1102109
- Pinho, S. S., Oliveira, P., Cabral, J., Carvalho, S., Huntsman, D., Gärtner, F., et al. (2012). Loss and recovery of Mgat3 and GnT-III mediated E-cadherin N-glycosylation is a mechanism involved in epithelial-mesenchymal-epithelial transitions. *PLoS ONE* 7:e33191. doi: 10.1371/journal.pone.0033191
- Pouyssegur, J., Dayan, F., and Mazure, N. M. (2006). Hypoxia signalling in cancer and approaches to enforce tumour regression. *Nature* 441, 437–443. doi: 10.1038/nature04871
- Qin, Y., Zhong, Y., Dang, L., Zhu, M., Yu, H., Chen, W., et al. (2012). Alteration of protein glycosylation in human hepatic stellate cells activated with transforming growth factor- $\beta 1$. *J. Proteomics* 75, 4114–4123. doi: 10.1016/j.jpropt.2012.05.040

- Semenza, G. L. (2002). HIF-1 and tumor progression: pathophysiology and therapeutics. *Trends Mol. Med.* 8, S62–S67. doi: 10.1016/S1471-4914(02)02317-1
- Siegel, R. L., Miller, K. D., and Jemal, A. (2017). Cancer statistics, 2017. *CA Cancer J. Clin.* 67, 7–30. doi: 10.3322/caac.21387
- Soares, R., Balogh, G., Guo, S., Gärtner, F., Russo, J., and Schmitt, F. (2004). Evidence for the notch signaling pathway on the role of estrogen in angiogenesis. *Mol. Endocrinol.* 18, 2333–2343. doi: 10.1210/me.2003-0362
- Song, Y., Aglipay, J. A., Bernstein, J. D., Goswami, S., and Stanley, P. (2010). The bisecting GlcNAc on N-glycans inhibits growth factor signaling and retards mammary tumor progression. *Cancer Res.* 70, 3361–3371. doi: 10.1158/0008-5472.CAN-09-2719
- Tan, Z., Lu, W., Li, X., Yang, G., Guo, J., Yu, H., et al. (2014). Altered N-glycan expression profile in epithelial-to-mesenchymal transition of NMuMG cells revealed by an integrated strategy using mass spectrometry and glycogene and lectin microarray analysis. *J. Proteome Res.* 13, 2783–2795. doi: 10.1021/pr401185z
- Taniguchi, N., and Kizuka, Y. (2015). Glycans and cancer: role of N-glycans in cancer biomarker, progression and metastasis, and therapeutics. *Adv. Cancer Res.* 126, 11–51. doi: 10.1016/bs.acr.2014.11.001
- Wardi, L., Alaaeddine, N., Raad, I., Sarkis, R., Serhal, R., Khalil, C., et al. (2014). Glucose restriction decreases telomerase activity and enhances its inhibitor response on breast cancer cells: possible extra-telomerase role of BIBR 1532. *Cancer Cell Int.* 14:60. doi: 10.1186/1475-2867-14-60
- Xu, Q., Akama, R., Isaji, T., Lu, Y., Hashimoto, H., Kariya, Y., et al. (2011). Wnt/ β -catenin signaling down-regulates N-acetylglucosaminyltransferase III expression: the implications of two mutually exclusive pathways for regulation. *J. Biol. Chem.* 286, 4310–4318. doi: 10.1074/jbc.M110.182576
- Xu, Q., Isaji, T., Lu, Y., Gu, W., Kondo, M., Fukuda, T., et al. (2012). Roles of N-acetylglucosaminyltransferase III in epithelial-to-mesenchymal transition induced by transforming growth factor β 1 (TGF- β 1) in epithelial cell lines. *J. Biol. Chem.* 287, 16563–16574. doi: 10.1074/jbc.M111.262154
- Yoshimura, M., Ihara, Y., Matsuzawa, Y., and Taniguchi, N. (1996). Aberrant glycosylation of E-cadherin enhances cell-cell binding to suppress metastasis. *J. Biol. Chem.* 271, 13811–13815. doi: 10.1074/jbc.271.23.13811
- Yu, H., Zhu, M., Qin, Y., Zhong, Y., Yan, H., Wang, Q., et al. (2012). Analysis of glycan-related genes expression and glycan profiles in mice with liver fibrosis. *J. Proteome Res.* 11, 5277–5285. doi: 10.1021/pr300484j
- Yu, M., Zhao, Q., Shi, L., Li, F., Zhou, Z., Yang, H., et al. (2008). Cationic iridium (III) complexes for phosphorescence staining in the cytoplasm of living cells. *Chem. Commun.* 2115–2117. doi: 10.1039/b800939b
- Zhang, H., Akman, H. O., Smith, E. L., Zhao, J., Murphy-Ullrich, J. E., and Batuman, O. A. (2003). Cellular response to hypoxia involves signaling via Smad proteins. *Blood* 101, 2253–2260. doi: 10.1182/blood-2002-02-0629
- Zhong, H., Chiles, K., Feldser, D., Laughner, E., Hanrahan, C., Georgescu, M. M., et al. (2000). Modulation of hypoxia-inducible factor 1 α expression by the epidermal growth factor/phosphatidylinositol 3-kinase/PTEN/AKT/FRAP pathway in human prostate cancer cells: implications for tumor angiogenesis and therapeutics. *Cancer Res.* 60, 1541–1545.
- Zhou, G., Dada, L. A., Wu, M., Kelly, A., Trejo, H., Zhou, Q., et al. (2009). Hypoxia-induced alveolar epithelial-mesenchymal transition requires mitochondrial ROS and hypoxia-inducible factor 1. *Am. J. Physiol. Lung Cell. Mol. Physiol.* 297, L1120–L1130. doi: 10.1152/ajplung.00007.2009

Conflict of Interest Statement: The authors declare that the research was conducted in the absence of any commercial or financial relationships that could be construed as a potential conflict of interest.

The handling editor is currently co-organizing a Research Topic with one of the authors FG, and confirms the absence of any other collaboration.

Copyright © 2018 Tan, Wang, Li and Guan. This is an open-access article distributed under the terms of the Creative Commons Attribution License (CC BY). The use, distribution or reproduction in other forums is permitted, provided the original author(s) and the copyright owner are credited and that the original publication in this journal is cited, in accordance with accepted academic practice. No use, distribution or reproduction is permitted which does not comply with these terms.